INTRODUCTION OF A POSSIBLE APPROACH TO MODELLING THE PROPAGATION OF HEAD CHECK CRACKS USING THE EXTENDED FINITE ELEMENT METHOD TAKING INTO ACCOUNT FLUID PENETRATION

Dániel Bóbis*
Péter T. Zwierczyk
Department of Machine and Product Design
Faculty of Mechanical Engineering
Budapest University of Technology and Economics
Műegyetem rkp. 3., H-1111 Budapest, Hungary
E-mail: bobis.daniel.@gt3.bme.hu
*Corresponding author

KEYWORDS
Rolling contact fatigue (RCF), head check (HC), eXtended Finite Element Method (X-FEM), crack growth simulation, stress intensity factor (SIF), Ansys Mechanical APDL, crack propagation, railway rail.

ABSTRACT

This paper presents a possible modelling technique for the propagation of the so-called head check cracks. The term head check (HC) refers to a kind of multiple hairline cracking in the railhead caused by rolling contact fatigue (RCF). This phenomenon has become widespread in recent decades and is still a major problem for the rail industry. The aim of this study is to create a specific finite element model to examine head checks numerically in order to gain a better understanding of the behaviour of these cracks.

The paper summarizes the most important aspects of the phenomenon under study and outlines the methods used. Regarding the fatigue-based crack growth simulation, the Extended Finite Element Method was applied. The finite element analysis examines the development of the already-initiated cracks in the cross-section of the rail. The finite element model also takes into account the effect of fluid forced between cracks using a certain technique. The study aims to explore the possibilities of the modelling technique and to estimate the level at which the head check phenomenon can be examined from this approach. Consequently, the exact numerical value of the results might be less relevant, but the characteristics of the results may become rather more interesting.

Results achieved in the study have shown that the developed method can be used to examine the head check phenomenon, even if it needs further improvements. Overall, the modelling technique has potential and is a direction for further research in the future.

INTRODUCTION

Overview of the Examined Phenomenon

Over the last few decades, the number of rolling contact fatigue (RCF) related failures of railway tracks has increased significantly, including the appearance of head checks (HC). This can probably be attributed to the increasing demands, such as faster trains, more frequent traffic, higher axle loads etc. Many different solutions have been developed over time to treat the issue successfully. Some of these, for instance, are the optimal selection of rail steel grades, the use of special rail profiles and preventive maintenance. However, the phenomenon is still a major problem for the railway industry.

As illustrated in Figure 1, head checks can be identified as numerous of hairline cracks located parallel to each other at a slanted angle near the gauge corner of the railhead.

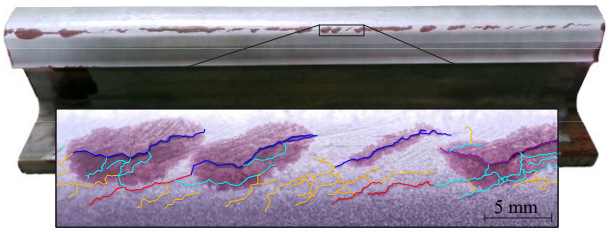

Figure 1: Typical HCs on a Part of a Rail. As a Result of a Former Liquid Penetrant Inspection, Cracks are Highlighted in Red. At the Bottom, Similar Cracks are Represented with the Same Color (Bóbis, 2022)

The HC failure usually occurs in passing tracks or curved rail sections, where the highest loads are experienced. The initiation of these cracks is related to the plastic deformation of the rail surface from concentrated loads of the wheel-rail connection. Due to plastic deformation, hammer-hardening effect occurs on the upper layers of the rail, which causes the steel to harden significantly while its elasticity declines. This is the main mechanism of how these microcracks are initiated.

Communications of the ECMS, Volume 37, Issue 1,
Proceedings, ©ECMS Enrico Vicario, Romeo Bandinelli,
Virginia Fani, Michele Mastroianni (Editors) 2023
ISBN: 978-3-937436-80-7/978-3-937436-79-1 (CD) ISSN 2522-2414

Fluid entering between the cracks has an important impact on the growth of the cracks that have already been initiated (Figure 2).

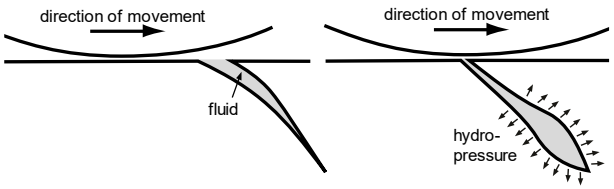

Figure 2: Mechanism of Crack Propagation by The Pressure of a Trapped Fluid (Ekberg, 2005)

As Figure 2 depicts, the opening of the cracks can be closed by the rolling wheel, and the loads passing through the trapped fluid create a significant hydrostatic pressure which tends to open the crack. Thus, this mechanism is an important factor in the progress of crack propagation.

The appearance of a head check becomes problematic because, if not handled in time properly, it can lead to even more severe defects. Typically, it causes spalling of the rail surface, which results in a strong negative impact on the dynamic behaviour of the rolling stock and generates unnecessary loads on the sensitive mechanical components of the vehicles. They can even cause the fracture of the entire cross-section of the rail in extreme cases. Therefore, it is particularly important to detect and treat the damage properly.

The problem under discussion is even more complex because it is not easy to detect. For the detection of HC defects, typically eddy current based measuring devices are used. However, their accuracy and reliability may be questionable in some cases.

The treatment of an already evolved HC formation can be achieved by removing the damaged layers of the rail, typically by some grinding process. However, these processes are highly expensive, thus the extent and frequency of the maintenance is a critical question. Therefore, treating HC defects properly is not only for safety reasons, but also very important from an economic point of view as well.

Methods

The Extended Finite Element Method was used for the analyses, which allows even such specific phenomena to be modelled as crack propagation. The main concept of the method is, briefly, that the degrees of freedom of the displacement field is extended, and special shape functions are introduced. This is how the method describes different discontinuities, in this particular study the effect of cracks. The method describes the cracks independently from the finite element mesh. The most important and outstanding advantages of this approach are due to this particular approach: it does not require a complicated adaptive regeneration of the mesh, nor does it require such a drastic mesh refinement at the critical locations as in the classical finite element method (Koei, 2015).

The quantities calculated numerically by the X-FEM are primarily the stress intensity factors (SIFs), denoted by *K*. These are interpreted as shown in Figure 3. Mode I crack opening is associated with K_1, Mode II and Mode III with K_2, K_3 respectively.

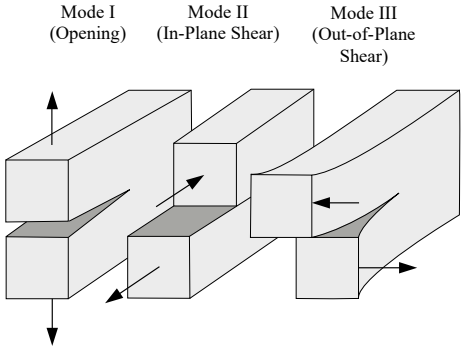

Figure 3. Crack Loading Modes (Anderson, 2005)

The equivalent stress intensity factor is calculated by the form

$$\Delta K_{\mathrm{eqv}} = \frac{1}{2}\cos\left(\frac{\Theta}{2}\right)\left[\left(\Delta K_1(1+\cos\Theta)\right) - 3\Delta K_2 \sin\Theta\right] \qquad (1)$$

where

$$\Delta\Theta = \Theta(K_1, K_2) \qquad (2)$$

indicates the instantaneous direction of crack propagation

Fatigue-based calculations are based on the Paris-Erdogan equation:

$$\frac{\mathrm{d}a}{\mathrm{d}N} = C\left(\Delta K_{\mathrm{eqv}}\right)^m, \qquad (3)$$

where

a:	crack length	[mm],
N:	number of cycles	[1],
C:	material constant	[1],
m:	material constant	[1].

FINITE ELEMENT MODEL

The X-FEM model presented below builds on the experience of previous studies (Bóbis, 2022). Earlier studies have already successfully applied the X-FEM to model HC cracks, but only at a rudimentary level with gross neglect. The aim was to create a model that is more accurate, with more cracks defined in the cross-section of the rail and taking into account the effect of the fluid.

Geometry

The geometry examined is a cross-section of a UIC 60 rail. The two-dimensional geometry with its plane-strain behaviour assumes that the extent of the crack is relatively large and perpendicular to the section. Only the rail head was modelled, other parts of the rail profile were neglected. Furthermore, non-relevant fillets were simplified. The geometry that was finally examined is shown in Figure 4/a.

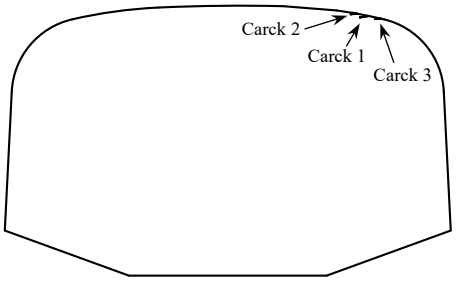

a) Simplified Railhead With Cracks

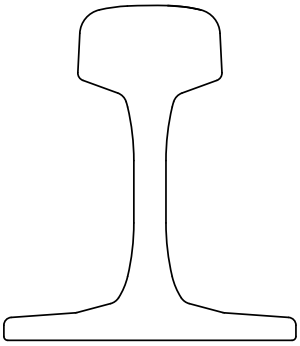

b) UIC 60 Rail Profile

Figure 4. Geometry Under Examination

The geometry contains three initial cracks, shown in Figure 5. The subject of this study is the development of these already-initiated cracks.

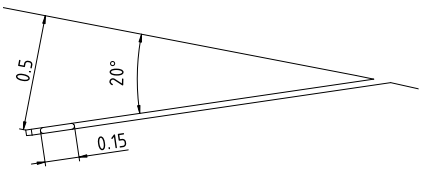

a) Crack 1

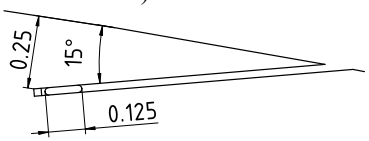

b) Crack 2

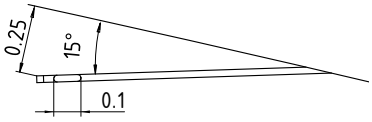

c) Crack 3

Figure 5. Main Dimensions of the Cracks

Finite Element Mesh

The finite element mesh contains four-node quadrilateral elements, as shown in Figure 6. The edge lengths of the elements are 1; 0.025; 0.0075 mm. Thus, the model contains a total of 40 786 elements.

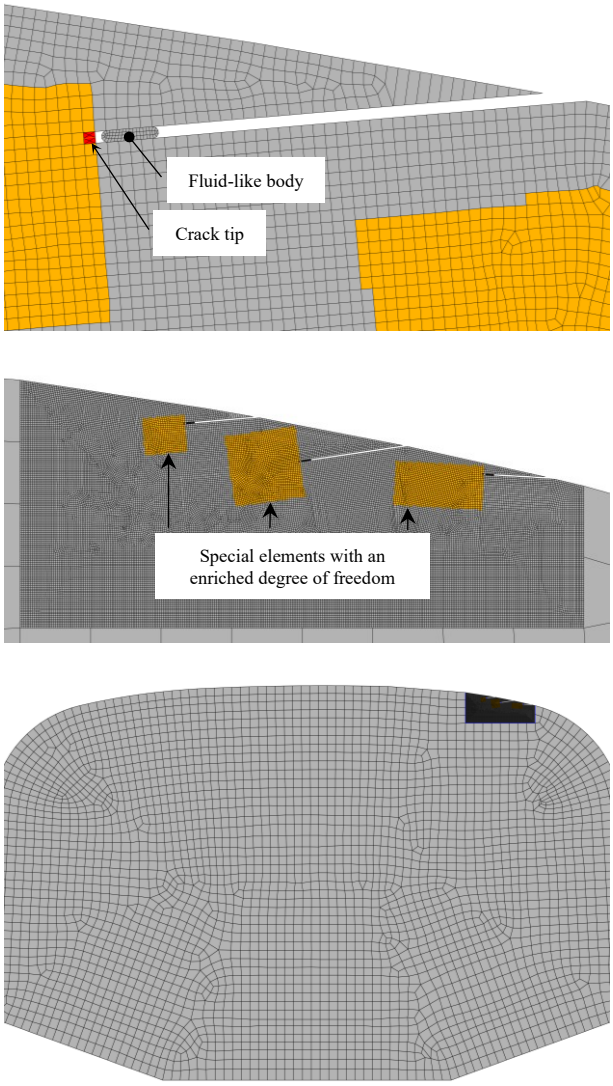

Figure 6. Finite Element Mesh

Elements highlighted in orange in Figure 6 are special and have an enriched degree of freedom, thus they can crack. The red element represents the instantaneous crack tip as Figure 6 shows.

A bonded mesh was created at the gauge corner of the railhead. The connection between the edges of the initial cracks is frictional, with a frictional coefficient of 0.15. The bottom of the inserted fluid-like bodies and the initial cracks are bonded by MPC algorithm (multipoint constraint). The connection between the top edge of the inserted fluid-like body and the initial crack is frictionless. All three cracks have the same contact parameters.

Material Properties

The material model is homogeneous linear elastic and isotropic. The material properties are summarized in Table 1.

Table 1. Material Properties

Name	Value	Unit
Bulk modulus of the fluid	2.2	GPa
C material constant	10^{-8}	1
m material constant	1.13	1
Poisson ratio (fluid)	0.4999	1
Poisson ratio (global)	0.3	1
Young's modulus of the inserted fluid-like bodies	3 301	1
Young's modulus (Global)	200 000	MPa

Since Young's modulus can not be interpreted for liquids, but it is the only way to define material properties in the model, this quantity is derived from the bulk modulus using the following relationship

$$K = \frac{E}{3 \cdot (1 - 2\nu)}, \tag{4}$$

where E is Young's modulus, ν is Poisson's ratio, and K is the bulk modulus. The properties of the fluid-like bodies are assumed to behave as ideal liquids and to have the room temperature parameters of water. Thus, Young's modulus of water can be expressed from equation (4).

The global material properties correspond to bainitic rail steel.

Loads and Boundary Conditions

The loads and boundary conditions are illustrated in Figure 7. At the bottom, all degrees of freedom are fixed. A linearly distributed surface pressure is defined on the marked part of the gauge corner.

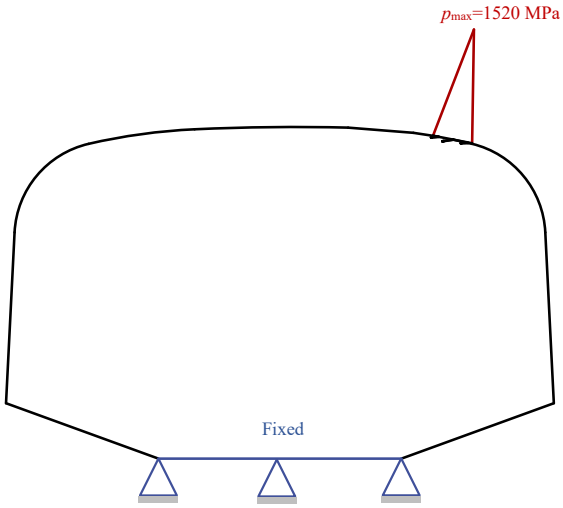

Figure 7. Boundary Conditions and Loads

The maximum value of the contact pressure and the extent of the wheel-rail contact area were chosen based on literature values (Figure 8 and Table 2). The radius of the wheel profile is 460 mm, and the radius of curvature of the rail profile is 330 mm.

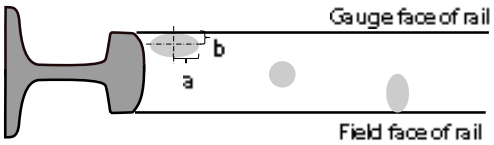

Figure 8. Interpretation of the Semi-axes of the Ellipse of the Contact Domain. (Esveld, 2001)

Table 2. Parameters of the Contact Ellipse and Compressive Stresses Due to 60 kN (Esveld 2001)

R_{wheel} [mm]	$R_{wheelprof}$ [mm]	$R_{railprof}$ [mm]	a [mm]	b [mm]	σ_N [MPa]
460	∞	300	6.1	4.7	1012
460	-330	300	3.9	14.6	502
460	-330	80	7.1	2.7	1520
150	-330	80	4.2	3.3	2103

RESULTS

Stationary Crack Analysis

The results of Stationary Crack Analysis are shown in Figure 9 and Figure 10. in true scale. The maximum deformation was found to be 0.1 mm, which resulted from the closing of the crack opening.

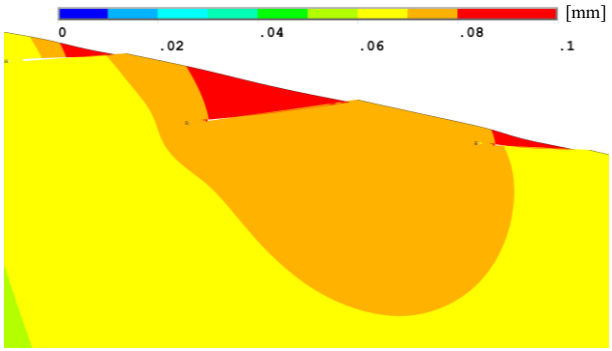

Figure 9. Displacement Field Around Cracks

The von Mises equivalent stress distribution is shown in Figure 10. The extremely high values are due to the linearly elastic material model and because the crack tip is a singular point. The circularly high stress values observed at the crack tips can also be considered as numerical errors, since this is the boundary of the region where the singularities are calculated (the outermost contour).

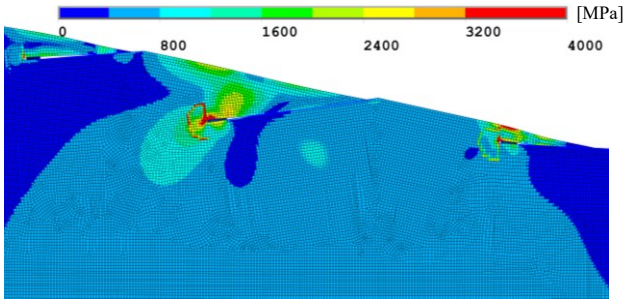

Figure 10. Von Mises Stress Distribution

The quantities are calculated along eight different Γ contours at the crack tips. The Γ contour is interpreted as in Figure 11, where n is the normal of the curve and e_1, e_2 are the axes of the coordinate system at the crack tip. The radius of the outermost contour is 0.15 mm.

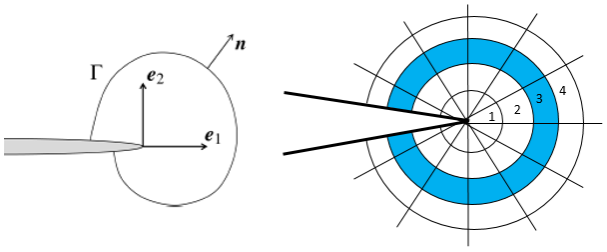

Figure 11. Interpretation of the Contours

As a result, the stress intensity factors were obtained according to Figure 12. For better clarity, only the first 10 pseudo-time domains (SET) are shown. The total analysis consists of 30 pseudo-time steps. On the charts shown below, K_1 is illustrated, but K_2 has the same trend. K_3 is not relevant due to the 2D model.

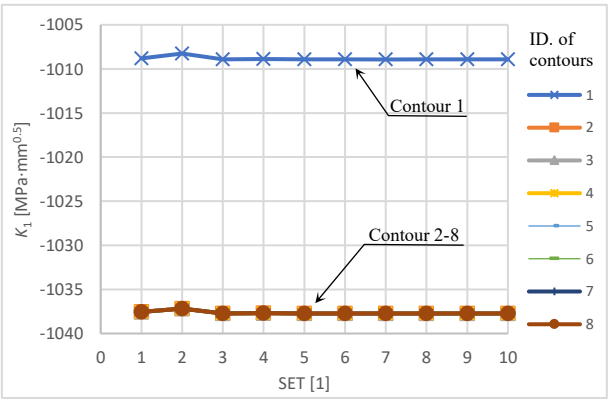

a) Crack 1

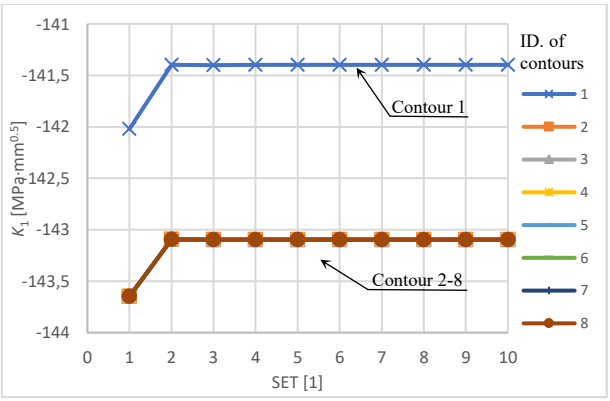

b) Crack 2

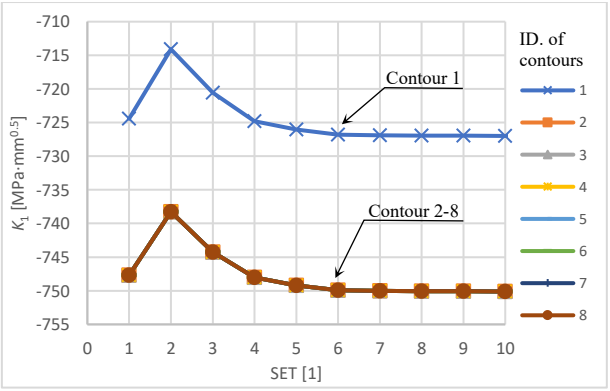

c) Crack 3

Figure 12. Results of the Stationary Crack Analysis

All three graphs show that the values of the first contour are slightly different. This is due to the singularity of the crack tip. To reduce the impact of the numerical error, the algorithm averages the results calculated on the 1-8 contours. Along contours 2-8, the results agree with high accuracy and quickly converge to a constant value, so the quality of the finite element mesh and model configuration is adequate.

Fatigue Crack-Growth Analysis

Regarding the fatigue-based crack growth analysis, the cracks developed as Figure 14 shows. The direction of growth of Crack 1 and Crack 3 is the same as the direction of the initial crack cut into the geometry. The reason for this is that the crack-opening effect of the inserted fluid-like bodies is not sufficiently effective; in other words, the propagation of the crack was inhibited. Although the elements cracked due to the algorithm, the value of the equivalent stress intensity factor, which is the basis of the crack growing, was actually zero during the analysis. Crack 2, on the other hand, turned and took a characteristic direction. after a while. Results of the stress intensity factors for Crack 2 during the analysis are shown in Figure 13.

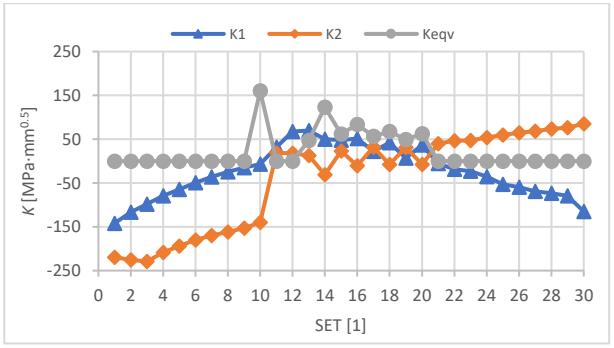

Figure 13. Stress Intensity Factors of Crack 2

The crack grows when the K_{eqv} value is large. K_{eqv} is calculated according to equation (1) and is mainly influenced by the sign of K_I. SIFs belonging to Crack 1 and Crack 3 are shown in Figure 14. Their equivalent stress intensity factors were zero, as mentioned earlier.

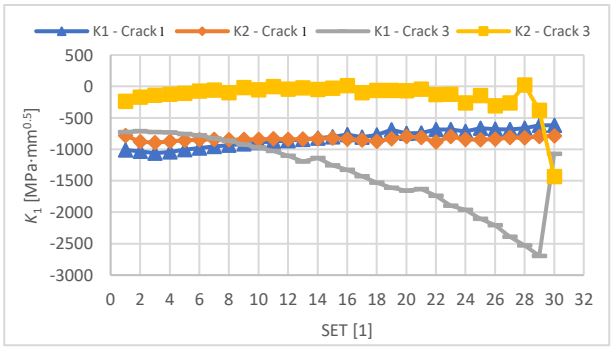

Figure 15. Stress Intensity Factors of Crack 1, Crack 3

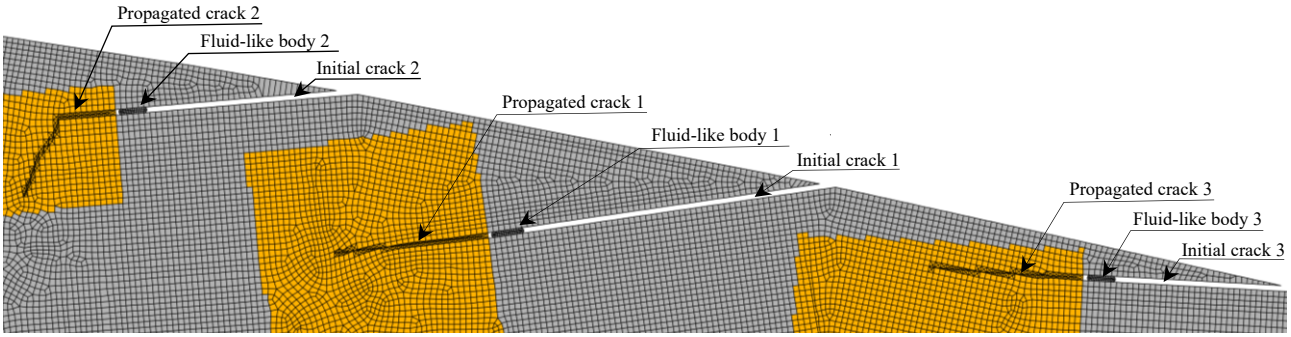

Figure 14. Result of the Fatigue Crack Growth Analysis

Based on the Paris-Erdogan equation, using the numerically calculated K_{eqv} and the crack increments resulting from the cracking of the finite elements, the rate of crack propagation can be calculated. This is shown in Figure 16.

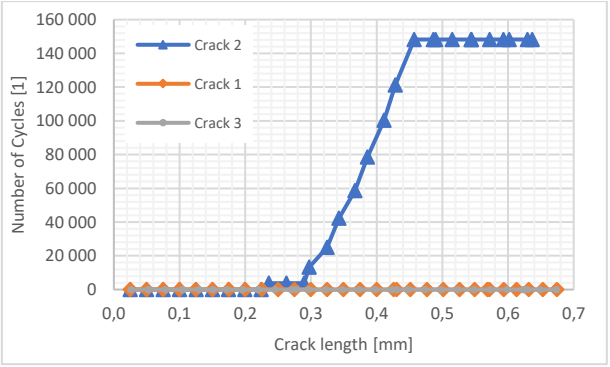

Figure 16. Lifetime Estimation

Since the K_{eqv} values the Crack 1 and Crack 3 were zero, therefore the lifecycle estimation curve is relevant only for Crarck 2. The same can be read from the curve, that the crack only grew in a relatively narrow range, almost linearly. The values presented are illustrative and may not reflect the real behaviour of the cracks.

CONCLUSIONS

During the Fatigue Crack-Growth analysis regarding Crack 1 and Crack 3, the crack opening effect of the inserted fluid-like bodies was not achieved. This implies that the compression of the cracked surfaces was dominant so that crack propagation was blocked. The crack opening effect was achieved only at Crack 2 which crack is located at the boundary of the contact region. So the effect of the fluid inside these cracks was managed to model properly only in some cases by this technique.

Although modelling the impact of fluids in this way was successful only in some cases, it also revealed that the real problem might not be as straightforward as it may appear. Indeed, in practice, the fluid may not always have this kind of strong crack opening effect, as liquids can easily escape or become the crack propagation blocking compression dominant and so on.

It is important to emphasize that this modelling approach is valid only for small crack growths since the bodies inserted do not follow the crack path, so their effect declines as the crack evolves. Furthermore, the geometry and position of these inserted bodies may also have a significant impact on the results.

As for further improvements, the loading model should be more precise. The Hertz pressure distribution should be used at the contact region, or even the relevant pressure values should be imported from another contact analysis. Furthermore, based on experiences, defining moving loads as in previous studies (Bóbis, 2022) may be more suitable. It would also be reasonable to apply the hydro-pressure directly onto the cracked elements, if possible, in practice. Beyond these improvements, it would be important to examine more geometrical conditions.

In the future, validation of the results with physical experiments is, of course, essential as well. It would also be valuable to compare numerical results with the experimental and known results. This means, on the one hand, the results of official data that can be retrieved and, on the other hand, the results of other kinds of examinations.

SUMMARY

In this study, a possible approach for modelling the head check phenomenon is presented. Head check is a kind of multiple hairline cracking on the rail head, which can cause serious problems for the railway industry.

The development of these cracks is significantly affected by the fluids entering and trapping between the cracks. The X-FEM model presented in this paper takes this fact into account by adding special bodies to the inside of the cracks that imitate the effect of fluids. The analysis covers stationary and fatigue-based crack propagation. As a result, the variation of stress intensity factors was obtained in detail in accordance with the development of the cracks. Furthermore, life-cycle estimations that are based on these results have been calculated.

Results suggested that the hydro-pressure arising in cracks may be substitutable with special inserted bodies only in certain cases and with compromises. However, they also demonstrated that the impact of fluids on the development of head checks inside these cracks might not be that simple to predict and handle in reality as well.

ACKNOWLEDGEMENTS

Project no. TKP-6-6/PALY-2021 has been implemented with the support provided by the Ministry of Culture and Innovation of Hungary from the National Research, Development and Innovation Fund, financed under the TKP2021-NVA funding scheme.

REFERENCES

Anderson, T. L. 2005. “Fracture Mechanics: Fundamentals and Applications”. Boca Raton: CRC Press. 640 p. ISBN 978-1-4200-5821-5.

Bobis D., Zwierczyk T. P., Mate T. 2022. “Application of the Extended Finite Element Method in the Aim of Examination of Crack Propagation in Railway Rails.” *Communications of the ECMS* , Volume 36, Issue 1. ISSN: 2522-2422. https://doi.org/10.7148/2022-0210

Ekberg A. and Kabo E. 2005. “Fatigue of railway wheels and rails under rolling contact and thermal loading—an overview.” *Wear*, Volume 258, Issues 7–8, Pages 1288-1300, ISSN 0043-1648.

Esveld C. 2001. “Modern Railway Track Zaltbommel.” MRT-Productions. 654 p. ISBN 90-800324-3-3

Khoei A. R 2015. ‘’Extended Finite Element Method: Theory and Applications’’. Pondicherry: SPi Publisher Services. 584 p. ISBN 978-1-118-45768-9.

AUTHOR BIOGRAPHIES

DÁNIEL BÓBIS is a PhD student at the Budapest University of Technology and Economics Department of Machine and Product Design, where he received his MSc degree in mechanical engineering. His research field is the rolling contact fatigue caused crack propagation. His email address is bobis.daniel@gt3.bme.hu

PÉTER T. ZWIERCZYK is the deputy head of the Department of Machine and Product Design and assistant professor at Budapest University of Technology and Economics, where he received his M.Sc. degree and then completed his PhD in mechanical engineering. His main research field is the railway wheel-rail connection. He is a member of the finite element modelling (FEM) research group. His e-mail address is z.peter@gt3.bme.hu.